

## Test of the State Reduction Rule

G. M. D'Ariano,<sup>1,2</sup> Prem Kumar,<sup>1</sup> C. Macchiavello,<sup>2</sup> L. Maccone,<sup>2</sup> and N. Sterpi<sup>2</sup>

<sup>1</sup>*Department of Electrical and Computer Engineering, Northwestern University,  
2145 North Sheridan Road, Evanston, Illinois 60208-3118*

<sup>2</sup>*Dipartimento di Fisica "A. Volta" and Istituto Nazionale di Fisica della Materia, Via Bassi 6, 27100 Pavia, Italy  
(Received 11 December 1998)*

We present an experiment for testing quantum state reduction. The state reduction rule is tested using optical homodyne tomography by directly measuring the fidelity between the theoretically expected reduced state and the experimental state.

PACS numbers: 03.65.Bz, 42.50.-p

In quantum mechanics state reduction (SR) is still a very discussed rule. The so-called "projection postulate" was introduced by von Neumann [1] to explain the results from the Compton-Simons experiment, and it was generalized by Lüders [2] for measurements of observables with degenerate spectrum. The consistency of the derivation of the SR rule and its validity for generic measurements have been analyzed with some criticism [3]. In a very general context, the SR rule was derived in a physically consistent way from the Schrödinger equation for the composite system of object and measuring apparatus [4]. An experiment for testing quantum SR is therefore a very interesting matter. Such a test in general is *not* equivalent to a test of the repeatability hypothesis since the latter holds only for measurements of observables that are described by self-adjoint operators. For example, joint measurements like the Arthurs-Kelly one [5] are not repeatable, as the reduced states are coherent states, which are not orthogonal.

Quantum optics offers a possibility of testing the SR, because several observables can be chosen to perform different measurements on a fixed system. For instance, one can decide to perform either homodyne or heterodyne, or photon-number detection. To our knowledge this is a unique opportunity; in contrast, in particle physics the measurements are mostly quasiclassical and restricted to only a few observables. In addition, optical homodyne tomography (OHT), which is a powerful tool for measuring the density operator of the radiation field, has been developed in recent years [6] and it allows a precise determination of the quantum system after the SR.

A scheme for testing the SR could be based on tomographic measurements of the radiation density matrix after nondemolition measurements. However, such a scheme would reduce the number of observables that are available for the test. Instead, one can take advantage of the correlations between the twin beams produced by a nondegenerate optical parametric amplifier (NOPA), in which case one can test the SR even for demolitive-type measurements. Indeed, if a measurement is performed on one of the twin beams, the SR can be tested by homodyne tomography on the other beam.

Our scheme for the SR test is given in Fig. 1 (for the experimental setup, see the end of the paper). Different

kinds of measurements can be performed on beam 1: in this paper we show in detail the SR for heterodyne detection as well as photon-number detection, but any other kind of detection (such as homodyne or phase detection by heterodyne) could be considered.

The radiation state of the twin beams produced by a NOPA with vacuum input (i.e., spontaneous parametric down-conversion) can be written as

$$|\xi\rangle = V(k) |0\rangle |0\rangle = (1 - |\xi|^2)^{1/2} \sum_{n=0}^{\infty} \xi^n |n\rangle |n\rangle, \quad (1)$$

where  $V(k) = \exp[k(\hat{a}_1^\dagger \hat{a}_2^\dagger - \hat{a}_1 \hat{a}_2)]$  (for real  $k$ ) describes the action of the parametric amplifier having a gain parameter  $\xi = \tanh(k)$ . The subscripts 1 and 2 refer to operators of beams 1 and 2 with  $\hat{a}^\dagger$  and  $\hat{a}$  being the creation and annihilation operators of the field mode, respectively.

Before calculating the SR, we briefly recall the concept of probability operator-valued measure (POVM). For a

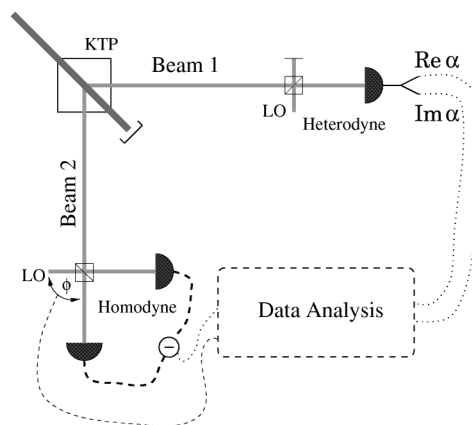


FIG. 1. Schematic of the proposed scheme for testing the SR for heterodyne detection. A NOPA generates a pair of twin beams (1 and 2). After heterodyning beam 1, the reduced state of beam 2 is analyzed by OHT, which is conditioned by the heterodyne outcome. In place of the heterodyne detector one can put any other kind of detector for testing the SR on different observables. In this paper we also consider the case of direct photodetection.

system described by a density operator  $\hat{\rho}$ , the probability  $p(\lambda)d\lambda$  that the outcome of a quantum measurement of an observable is in the interval  $[\lambda, \lambda + d\lambda]$  is given by Born's rule  $p(\lambda)d\lambda = \text{Tr}[\hat{\rho}\hat{P}_\lambda d\lambda]$ , where  $\hat{P}_\lambda d\lambda$  is the POVM pertaining to the measurement (such that  $\hat{P}_\lambda \geq 0$  and  $\int d\lambda \hat{P}_\lambda = \hat{1}$ ). For an exact measurement of an observable, which is described by a self-adjoint operator,  $\hat{P}_\lambda$  is just the projector over the eigenvector corresponding to the outcome  $\lambda$ . In the case of the photon number  $\hat{a}^\dagger \hat{a}$  the spectrum is discrete and the POVM is  $\hat{P}_m = |m\rangle\langle m|$  for integer eigenvalue  $m$ . For the Arthurs-Kelly joint measurement of the position and momentum (corresponding to a joint measurement of the two quadratures of the field) we have  $\hat{P}_\alpha = \pi^{-1}|\alpha\rangle\langle\alpha|$ , where  $|\alpha\rangle$ ,  $\alpha \in \mathbb{C}$ , is a coherent state, i.e.,  $\hat{a}|\alpha\rangle = \alpha|\alpha\rangle$ .

Now let us analyze the SR for our scheme. When on beam 1 we perform a measurement described by  $\hat{P}_\lambda$ , the reduced normalized state of beam 2 is

$$\hat{\rho}(\lambda) = \frac{\text{Tr}_1[|\xi\rangle\langle\xi|(\hat{P}_\lambda \otimes \hat{1})]}{\text{Tr}_{1,2}[|\xi\rangle\langle\xi|(\hat{P}_\lambda \otimes \hat{1})]} = \frac{\hat{\Xi}\hat{P}_\lambda^*\hat{\Xi}^\dagger}{p(\lambda)}, \quad (2)$$

where  $\hat{\Xi} = (1 - |\xi|^2)^{1/2} \xi^{\hat{a}^\dagger \hat{a}}$ , and  $p(\lambda) = \text{Tr}_{1,2}[\hat{\Xi}\hat{P}_\lambda^*\hat{\Xi}^\dagger]$  is the probability density of the measurement outcome  $\lambda$ . In the limit of infinite gain ( $\xi \rightarrow 1$ )  $\hat{\rho}(\lambda) \propto \hat{P}_\lambda^*$ ; for example, for heterodyne detection with outcome  $\alpha$ , we have  $\hat{\rho}(\alpha) = |\alpha^*\rangle\langle\alpha^*|$ .

If the readout detector on beam 1 has quantum efficiency  $\eta_r$ , then according to the SR rule the state in beam 2 is

$$\hat{\rho}^{\eta_r}(\lambda) = \frac{\hat{\Xi}(\hat{P}_\lambda^{\eta_r})^*\hat{\Xi}^\dagger}{p^{\eta_r}(\lambda)}, \quad (3)$$

where  $p^{\eta_r}(\lambda) = \text{Tr}_{1,2}[\hat{\Xi}(\hat{P}_\lambda^{\eta_r})^*\hat{\Xi}^\dagger]$ , and  $\hat{P}_\lambda^{\eta_r}$  is the POVM for measurement with a nonunit quantum efficiency. For heterodyne detection one has [7]

$$\hat{P}_\alpha^{\eta_r} = \frac{1}{\pi} \int \frac{d^2z}{\pi\Delta_{\eta_r}^2} e^{-\frac{|z-\alpha|^2}{\Delta_{\eta_r}^2}} |z\rangle\langle z|, \quad (4)$$

where  $\Delta_{\eta_r}^2 = (1 - \eta_r)/\eta_r$ , and  $\eta_r$  is the overall quantum efficiency of the heterodyne detector. For direct photodetection the ideal POVM  $\hat{P}_m = |m\rangle\langle m|$  is modified to [7]

$$\hat{P}_m^{\eta_r} = \sum_{j=m}^{\infty} \binom{j}{m} \eta_r^m (1 - \eta_r)^{j-m} |j\rangle\langle j|. \quad (5)$$

The experimental test proposed in this paper consists of performing conditional homodyne tomography on beam 2, given the outcome  $\lambda$  of the measurement on beam 1. Actually, through homodyne tomography we can directly measure the ‘‘fidelity of the test’’

$$F(\lambda) = \text{Tr}[\hat{\rho}^{\eta_r}(\lambda)\hat{\rho}_{\text{meas}}(\lambda)], \quad (6)$$

where  $\hat{\rho}^{\eta_r}(\lambda)$  is the theoretically expected state in Eq. (3), and  $\hat{\rho}_{\text{meas}}(\lambda)$  is the experimentally measured state of beam 2. Notice that in Eq. (6) we use the term fidelity even if  $F(\lambda)$  is a proper fidelity when at least one of the two states is pure, which occurs in the limit of unit quantum efficiency  $\eta_r$ . In the following we evaluate the

theoretical value of the fidelity  $F(\lambda)$  and compare it with the simulation of the tomographically measured value.

The fidelity (6) can be directly measured by OHT with use of the kernel function for the operator  $\hat{\rho}^{\eta_r}(\lambda)$ , as it can be done for the expectation value of any (generally complex) operator of the field mode [8]. In fact, for a generic operator  $\hat{O}$ , the expectation value  $\langle\hat{O}\rangle$  can be measured by averaging the kernel function  $\mathcal{R}_{\eta_h}[\hat{O}](x, \phi)$  over the homodyne data, namely,

$$\langle\hat{O}\rangle = \int_0^\pi \frac{d\phi}{\pi} \int_{-\infty}^{+\infty} dx p_{\eta_h}(x, \phi) \mathcal{R}_{\eta_h}[\hat{O}](x, \phi), \quad (7)$$

where  $\eta_h$  is the overall quantum efficiency of the homodyne detector, and  $p_{\eta_h}(x, \phi)$  is the probability distribution of the quadrature  $\hat{x}_\phi = (a^\dagger e^{i\phi} + a e^{-i\phi})/2$  at phase  $\phi$  relative to the local oscillator (LO). In Ref. [8] the kernel function for a generic operator  $\hat{O}$  is derived, with the following result:

$$\mathcal{R}_{\eta_h}[\hat{O}](x, \phi) = \int_0^{+\infty} dk k e^{\frac{1-\eta_h}{8\eta_h} k^2} \times \text{Tr}\{\hat{O} \cos[k(x - \hat{x}_\phi)]\}. \quad (8)$$

Hence,  $F(\lambda)$  is obtained from an average of the form

$$F(\lambda) = \int_0^\pi \frac{d\phi}{\pi} \int_{-\infty}^{+\infty} dx p_{\eta_h}(x, \phi; \lambda) \times \mathcal{R}_{\eta_h}[\hat{\rho}^{\eta_r}(\lambda)](x, \phi), \quad (9)$$

where  $p_{\eta_h}(x, \phi; \lambda)$  is the conditional homodyne probability distribution for outcome  $\lambda$  at the readout detector.

For heterodyne detection of beam 1 with outcome  $\alpha \in \mathbb{C}$ , the reduced state of beam 2 according to the SR rule is given by the displaced thermal state

$$\hat{\rho}^{\eta_r}(\alpha) = \eta_\xi \hat{D}(\gamma) (1 - \eta_\xi)^{\hat{a}^\dagger \hat{a}} \hat{D}^\dagger(\gamma), \quad (10)$$

where

$$\eta_\xi = 1 + (\eta_r - 1)|\xi|^2, \quad \gamma = \frac{\xi \eta_r}{\eta_\xi} \alpha^*, \quad (11)$$

and  $\hat{D}(\gamma) = \exp(\gamma \hat{a}^\dagger - \gamma^* \hat{a})$  is the usual displacement operator. The kernel function for measuring  $F(\alpha)$  is easily calculated from Eqs. (8)–(11). One has

$$\mathcal{R}_{\eta_h}[\hat{\rho}^{\eta_r}(\alpha)](x, \phi) = \frac{2\eta_h \eta_\xi}{2\eta_h - \eta_\xi} \times \Phi\left(1, \frac{1}{2}; -\frac{2\eta_h \eta_\xi}{2\eta_h - \eta_\xi} (x - \gamma_\phi)^2\right), \quad (12)$$

where  $\gamma_\phi = \text{Re}(\gamma e^{-i\phi})$ , and  $\Phi(a, b; z)$  denotes the customary confluent hypergeometric function of argument  $z$ . The kernel in Eq. (12) is bounded for  $\eta_h > \frac{1}{2}\eta_\xi$ , i.e., for the fidelity measurement, one needs to satisfy the

following bound on the quantum efficiencies:

$$\eta_h > \frac{1}{2} [1 + |\xi|^2(\eta_r - 1)]. \quad (13)$$

As one can see from Eq. (13), for  $\eta_h > 0.5$  the fidelity can be measured for any value of  $\eta_r$  and any gain parameter  $\xi$  of the NOPA. We recall that the condition  $\eta_h > 0.5$  is required for the measurement of the density matrix of a radiation state [9]. However, in a direct measurement of the fidelity the measurement of the density matrix is bypassed and we see from Eq. (13) that the bound  $\eta_h = 0.5$  can be lowered.

The tomographically measured fidelity  $F(\alpha)$  in Eq. (9) with  $\hat{\rho}^{\eta_r}(\alpha)$  as given in Eq. (10) must be compared with

$$\mathcal{R}_{\eta_h}[\hat{\rho}^{\eta_r}(n)](x, \phi) = \frac{(\eta_\xi \partial_z)^n}{n!} \Big|_{z=0} \frac{2\eta_h \eta_\xi}{2\eta_h - \eta_\xi + z} \Phi\left(1, \frac{1}{2}; -\frac{2\eta_h(\eta_\xi - z)}{2\eta_h - \eta_\xi + z} x^2\right). \quad (16)$$

We see that the same bound, Eq. (13), on the quantum efficiencies holds true also for direct photodetection. In this case, the tomographically measured fidelity  $F(n)$  must be compared with the following theoretical value:

$$F_{\text{th}}(n) = \eta_\xi^{2+2n} F(2n+1, 2n+1; 1; (1-\eta_\xi)^2), \quad (17)$$

where  $F(a, b; c; z)$  denotes the customary hypergeometric function of argument  $z$ .

In Fig. 2 we report results of the tomographically measured fidelity for heterodyne detection on beam 1. The numerical results are obtained by simulating the quadrature probability distribution pertaining to the reduced state (10), and averaging the kernel functions in Eq. (12). The simulation is performed according to the SR hypothesis; thus the homodyne probability distribution in Eq. (9) corresponds to state (10). Notice that for heterodyne detection

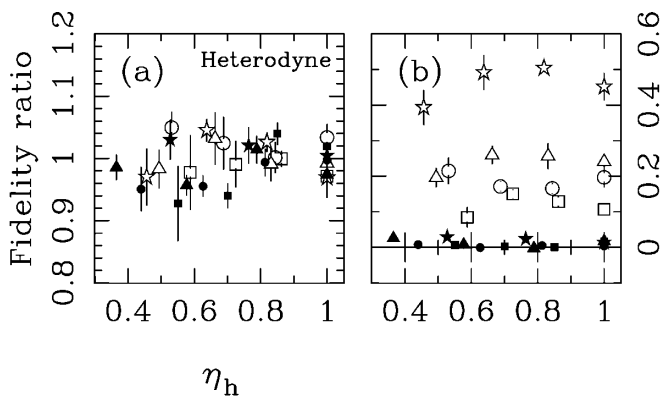


FIG. 2. (a) Fidelity ratio  $\bar{F}/F_{\text{th}}$  (see text) for heterodyne detection with quantum efficiency  $\eta_r = 0.8, 0.5, 0.3$ , and  $0.1$  (squares, circles, triangles, and stars, respectively). The open (solid) points are for  $\bar{n} = 1$  ( $\bar{n} = 100$ ) thermal photons per beam. The number of data used in each case is 2080 (4 blocks of 20 data samples for 26 settings of the phase  $\phi$ ). (b) Fidelity ratio from the same simulated homodyne data of (a), but for  $\bar{F}$  with a reduced state with opposite amplitude ( $\alpha \rightarrow -\alpha$ ) in Eq. (11).

the theoretical value

$$F_{\text{th}}(\alpha) = \eta_\xi / (2 - \eta_\xi). \quad (14)$$

Notice that  $F_{\text{th}}(\alpha)$  does not depend on  $\alpha$ : therefore in the following it will be simply denoted by  $F_{\text{th}}$ .

Now we analyze the SR for direct photodetection of beam 1. For an outcome  $n$  at the readout photodetector, the reduced state of beam 2 is given by

$$\hat{\rho}^{\eta_r}(n) = \eta_\xi \left( \frac{\eta_\xi}{1 - \eta_\xi} \right)^n \binom{\hat{a}^\dagger \hat{a}}{n} (1 - \eta_\xi)^{\hat{a}^\dagger \hat{a}}. \quad (15)$$

The pattern function for the corresponding fidelity measurement is

the measurement spectrum is continuous and the probability  $p^{\eta_r}(\alpha)d\alpha$  of outcome  $\alpha$  is infinitesimal. Therefore, we present the average value  $\bar{F}$  of the fidelity  $F(\alpha)$  over  $p^{\eta_r}(\alpha)$ . Results for various values of the quantum efficiencies  $\eta_r$  and  $\eta_h$  are reported along with two different values of the NOPA gain parameter  $\xi$  [given in terms of the number of thermal photons per beam  $\bar{n} = |\xi|^2 / (1 - |\xi|^2)$ ]. For comparison in the same figure we also report the fidelity ratio as obtained from the same simulated homodyne data, but for mismatched state reconstruction corresponding to the experimental fidelity with a reduced state with opposite amplitude  $\alpha \rightarrow -\alpha$  in Eq. (11). One can clearly see that a decisive test can be performed with samples of a few thousand measurements only. The error in the measurement, denoted by the vertical error bars, is rather insensitive to both quantum efficiencies and the NOPA gain in the considered range of values. Notice, however, that the disagreement for the mismatched fidelity increases for improved quantum efficiency at the heterodyne  $\eta_r$  and for larger gain at the NOPA.

In Fig. 3 the tomographically measured fidelity is reported when direct photodetection is performed on beam 1. Here the simulation is achieved analogously to the previous case, but now using Eqs. (15) and (16). Results for various outcomes  $n$  are given with different values of  $\eta_h$  and  $\bar{n}$ . For comparison in the same figure we also report the fidelity ratio as obtained from the same simulated homodyne data, but for a mismatched state reconstruction corresponding to the experimental fidelity with the state from heterodyne state reduction in Eq. (10) with  $\alpha = \sqrt{\bar{n}}$ . Again, the test can be performed with samples of a few thousand measurements only; the resulting error in the measurement is rather insensitive to the values of the experimental parameters. Notice that the disagreement for the mismatched fidelity increases for larger outcomes  $n$ , where the fact that the fidelity is slightly improved for larger gain at the NOPA is an artifact due to the analytical form of the state for

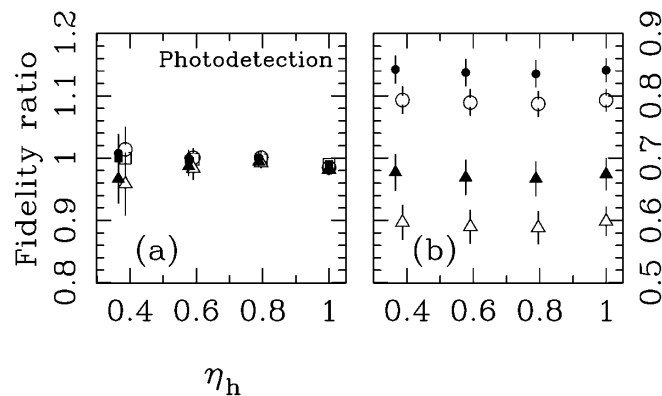


FIG. 3. (a) Fidelity ratio  $F(n)/F_{\text{th}}(n)$  (see text) for direct detection with quantum efficiency  $\eta_r = 0.3$ , resulting in outcomes  $n = 0, 1$ , and  $2$  at the photodetector (squares, circles, and triangles, respectively). The thermal photons per beam are  $\bar{n} = 10$  (open points) and  $\bar{n} = 100$  (solid points). In each case  $10^4$  data are used and the error bars are obtained by dividing the data into ten blocks. (b) Fidelity ratio from the same simulated homodyne data of (a), but with the experimental fidelity with the state from heterodyne state reduction in Eq. (10) with  $\alpha = \sqrt{\bar{n}}$ .

low efficiency  $\eta_r$ . Analogous results would have been obtained for the symmetrically mismatched case for Fig. 2.

In our lab the NOPA consists of a type-II phase-matched KTP crystal that is pumped by the second harmonic of a Q-switched and mode-locked Nd:YAG laser. Previously, we have employed such a NOPA, with parametric gains  $>10$  ( $|\xi|^2 > 0.9$ ), to generate highly quantum-correlated twin beams of light at 1064 nm [10]. By appropriately choosing the input quantum state, a similar setup was then used to demonstrate the production of squeezed-vacuum state with a high degree ( $5.8 \pm 0.2$  dB) of squeezing [11]. In the present context, the twin beams, which are easily separable because of their orthogonal polarizations resulting from type-II phase matching, can be separately detected; beam 2 with a homodyne detector for detecting the reduced quantum state and beam 1 with either a heterodyne detector or a photon-counting detector. We have recently reported preliminary results of double homodyne measurements [12], which were performed to reconstruct the joint photon-number density matrix of the twin-beam state [13]. The main challenge in the present experiment is the achievement of high degrees of overlap (mode-matching efficiency) between the down-converted and the LO modes. Such overlap is nontrivial in pulsed, traveling-wave experiments owing to the distortion of the down-converted modes that is caused by the spatiotemporally Gaussian profile of the pump beam. With suitable choice of LOs, however, we have previously obtained  $\eta_h > 0.70$  [14], an adequate value for the present experiment (cf. Figs. 2 and 3). In photon-counting measurements on beam 1, the main challenge will be the selection of the appropriate mode. Mode-selective photon count-

ing can be performed by passing beam 1 through an appropriate filter before photodetection. In addition, new high quantum-efficiency, solid-state photomultipliers have become available that can distinguish between  $0, 1, 2, \dots$  photons in ns-duration pulses [15].

In conclusion, we have presented an experiment to test the rule of state reduction upon quantum measurements. Our goal is achieved by changing the kind of measurement performed on one beam of a pair of twin beams. The reduced state of the other beam, which depends on the kind of measurement performed, is then experimentally observed through a tomographic measurement of the fidelity between the theoretically expected reduced state and the experimental state. We decided to present the test of SR in terms of the fidelity for illustrative purposes. However, the same test can be performed by tomographic reconstruction of the whole density matrix of the reduced state, without any modification in the schematic of the experiment.

This work has been supported by the U.S. Office of Naval Research and the PRA-CAT97 of the INFM.

- [1] J. von Neumann, *Mathematical Foundations of Quantum Mechanics* (Princeton University Press, Princeton, NY, 1955).
- [2] G. Lüders, *Ann. Phys. (Leipzig)* **8**, 322 (1951).
- [3] See, for example, E. P. Wigner, *Am. J. Phys.* **31**, 6 (1963); M. Ozawa, e-print Quant-Ph/9802022; N. Imoto, M. Ueda, and T. Ogawa, *Phys. Rev. A* **41**, 4127 (1990).
- [4] See M. Ozawa, *Ann. Phys. (N.Y.)* **259**, 121 (1997), and references therein.
- [5] E. Arthurs and J. L. Kelly, Jr., *Bell Syst. Tech. J.* **44**, 725 (1965).
- [6] G. M. D'Ariano, in *Quantum Optics and the Spectroscopy of Solids*, edited by T. Hakioglu and A. S. Shumovsky (Kluwer Academic Publishers, Dordrecht, The Netherlands, 1997), p. 175.
- [7] D'Ariano, in *Quantum Optics and the Spectroscopy of Solids* (Ref. [6]), p. 139.
- [8] G. M. D'Ariano, in *Quantum Communication, Computing and Measurement*, edited by O. Hirota, A. S. Holevo, and C. M. Caves (Plenum, New York and London, 1997), pp. 253–264.
- [9] G. M. D'Ariano and C. Macchiavello, *Phys. Rev. A* **57**, 3131 (1998).
- [10] O. Aytür and P. Kumar, *Phys. Rev. Lett.* **65**, 1551 (1990).
- [11] C. Kim and P. Kumar, *Phys. Rev. Lett.* **73**, 1605 (1994).
- [12] M. Vasilyev, S.-K. Choi, P. Kumar, and G. M. D'Ariano, in *Quantum Communication, Computing and Measurement II*, edited by P. Kumar, G. M. D'Ariano, and O. Hirota (Plenum, New York, to be published).
- [13] G. M. D'Ariano, M. Vasilyev, and P. Kumar, *Phys. Rev. A* **58**, 636 (1998).
- [14] O. Aytür and P. Kumar, *Opt. Lett.* **17**, 529 (1992).
- [15] M. D. Petroff, M. G. Stapelbroek, and W. A. Kleinmans, *Appl. Phys. Lett.* **51**, 406 (1987).